View metadata, citation and similar papers at core.ac.uk
brought to you by CORE
provided by Infoscience - École polytechnique fédérale de Lausanne

Zinc Tin Oxide as High-Temperature Stable Recombination Layer for Mesoscopic Perovskite/Silicon Monolithic Tandem Solar Cells

Jérémie Werner,[1] Arnaud Walter,[3] Esteban Rucavado,[1] Soo-Jin Moon,[3] Davide Sacchetto,[3] Michael Rienaecker,[2] Robby Peibst,[2] Rolf Brendel,[2] Xavier Niquille,[1] Stefaan De Wolf,[1, 4] Philipp Löper,[1] Monica Morales-Masis,[1] Sylvain Nicolay,[3] Bjoern Niesen,[1, 3] and Christophe Ballif [1, 3]

[1] *Ecole Polytechnique Fédérale de Lausanne (EPFL), Institute of Microengineering (IMT), Photovoltaics and Thin-Film Electronics Laboratory, Rue de la Maladière 71b, 2002 Neuchâtel, Switzerland*
[2] *Institute for Solar Energy Research Hamelin (ISFH), D-31860 Emmerthal, Germany*
[3] *CSEM, PV-Center, Jaquet-Droz 1, 2002 Neuchâtel, Switzerland*
[4] *Now at: King Abdullah University of Science and Technology (KAUST), KAUST Solar Center (KSC), Thuwal, 23955-6900, Saudi Arabia*

Perovskite/crystalline silicon tandem solar cells have the potential to reach efficiencies beyond those of silicon single-junction record devices. However, the high-temperature process of 500°C needed for state-of-the-art mesoscopic perovskite cells has, so far, been limiting their implementation in monolithic tandem devices. Here, we demonstrate the applicability of zinc tin oxide as recombination layer and show its electrical and optical stability at temperature up to 500°C. To prove the concept, we fabricate monolithic tandem cells with mesoscopic top cell with up to 16% efficiency. We then investigate the effect of zinc tin oxide thickness variation, showing a strong influence on the optical interference pattern within the tandem device. Finally, we discuss the perspective of mesoscopic perovskite cells for high-efficiency monolithic tandem solar cells.

Perovskite solar cells have made tremendous progress in a very short time, reaching now initial efficiencies above 22%.[1] In parallel to the single-junction development, perovskite materials were shown to have excellent properties for tandem applications, allowing for rapid advances, such that efficiencies beyond 20% on both monolithic and 4-terminal tandem architectures have already been reached,[2–5] with reported record 4 terminal measurements of 25.2%.[5]

So far, the research focused mainly on silicon heterojunction bottom cells,[3–5] as these devices combine record operating voltages with an excellent infrared response, and ease of contacting with a full TCO coverage on both sides of the device. However, due to their sensitivity to process temperature above 200-300°C,[6] this type of bottom cell is not compatible with high-efficiency *mesoscopic* perovskite top cells. Indeed, this perovskite cell architecture, which is at the origin of all recent single-junction efficiency certified records,[1,7–9] is commonly based on a mesoporous TiO_2 scaffold layer, which typically requires a 500°C annealing step, prior to perovskite absorber deposition. Most diffused silicon solar cells could be designed to be compatible with a 500°C step, as they undergo typical diffusion/oxidation or firing steps close to 900°C.

Incorporating this type of perovskite cell in a monolithic tandem therefore requires both silicon bottom cell and intermediate recombination layer to be stable up to a temperature of 500°C. Typical additional requirements for an efficient intermediate recombination layer are correct band energetics to guarantee efficient interband tunneling with the underlying silicon device, high optical transparency (especially between 600nm and 1200nm), as well as chemical stability and process simplicity.

Mailoa *et al.* demonstrated the use of a partially crystalline n^{++} *a*-Si / p^{++} *c*-Si tunnel junction made by plasma-enhanced chemical vapor deposition, which required a very careful control of the deposition conditions and post-deposition annealing.[2] In contrast, transparent conducting oxides (TCOs) have already proven their simplicity of application and effectiveness as recombination layers in monolithic tandem solar cells.[3–5] However, the commonly used indium tin oxide (ITO) or indium zinc oxide (IZO) are neither electrically nor optically stable upon annealing in oxygen containing environment at 500°C, and therefore are not compatible with the mesoscopic perovskite top cell fabrication procedure.

Here, we present a simple method to tandem a mesoscopic perovskite top cell with a homojunction silicon bottom cell, using a sputtered zinc tin oxide (ZTO) recombination layer. ZTO has previously been used as an electron transport layer in organic optoelectronic devices[10,11] and in thin-film transistors as the channel material.[12,13] It was shown to be a promising indium-free *n*-type metal oxide with high electron mobility and transparency, as well as good temperature stability and mechanical integrity.[14] These properties qualify ZTO as an attractive candidate for the integration in monolithic tandem devices as an intermediate

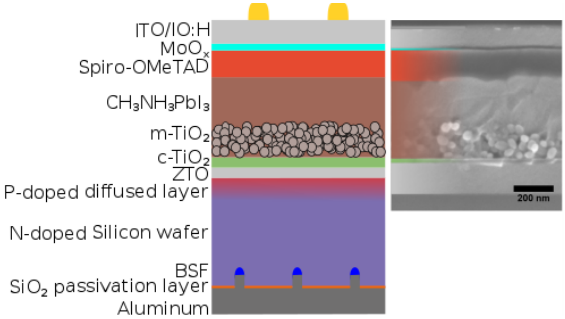

Figure 1 Monolithic tandem cell structure with mesoscopic perovskite top cell and homojunction silicon bottom cell. The SEM image shows a cross-section of a typical perovskite top cell. (BSF=Back Surface Field; m-TiO2 = scaffold layer; c-TiO2 = compact electron transport layer; Spiro-OMeTAD = hole transport layer)

recombination layer. In this article, we demonstrate the thermal stability of optical and electrical properties up to 500°C, suggesting that it can indeed be used effectively in a tandem solar cell as recombination layer. As a proof-of-principle, we fabricated monolithic tandem cells with efficiencies up to 16%, with an aperture area of 1.43 cm^2. Finally, we experimentally show how the variation of the recombination layer thickness influences the optical interference pattern in the device.

Bottom cell fabrication started with electrical junction formation in *n*-type silicon wafers. For this, silicon oxide layers were thermally grown on both wafer surfaces. The active device area was then defined by removing the oxide on the front side of the Si wafers, followed by boron implantation, forming thus a hole-collecting emitter. On the rear side, the surface-passivating silicon oxide layer was laser-patterned and phosphorus implanted for local contact and back surface field formation. We remark that the used wafers featured mirror-polished front sides (and a lapped back side), to avoid shunting of the solution processed top cell. To ensure the absence of a native SiO_2 layer, we performed a HF dip before the TCO (ITO or ZTO) was directly sputtered onto the boron-implanted silicon surface, followed by the perovskite top cell deposition. The top cell was composed of a sputtered compact TiO_2 layer (c-TiO_2), a TiO_2 scaffold layer (m-TiO_2) annealed at 500°C, a $CH_3NH_3PbI_3$ perovskite layer and a spiro-OMeTAD/MoO_x/IO:H/ITO top electrode, as described in more details in supplementary information and illustrated in Figure 1.

As ITO is one of the most commonly used TCOs in photovoltaics, it was naturally our initial choice for the intermediate recombination layer. However, strong degradation could be observed on finished monolithic tandem cells with poor current-voltage (*J-V*) characteristics, similar to the example shown in Figure 2a. Electrical characterization of the ITO layers on glass before and after annealing at 500°C showed a strong reduction in carrier density, which is attributed to a filling of the oxygen deficiencies, by oxygen diffusion from the air or from the capping TiO_2 layer. Consequently, a massive drop in conductivity from initially 2207 $(\Omega cm)^{-1}$ (mobility: 36.8 cm^2/Vs; carrier concentration: $3.7x10^{20}$ cm^{-3}; see Figure S6) could be observed, making the films essentially non-measurable with our Hall-effect setup after the complete annealing sequence. The strongly increased resistance in this recombination layer is believed to be responsible for the non-functional tandem devices.

In contrast, ZTO showed an improvement in the electrical and optical properties upon annealing at 500°C in air, as presented in Figure 3. After annealing, the film showed an improved total transmittance, up to 85% at a wavelength of 800 nm. The electrical properties were also enhanced, resulting in an increase in the Hall effect electron mobility from 21.8 to 35 $cm^2V^{-1}s^{-1}$ and an improvement in conductivity from 283 to 433 $(\Omega cm)^{-1}$, for 150-nm-thick layers on glass substrates. These properties are sufficient to ensure good transverse charge transport through a recombination junction.

We then applied this material in monolithic tandem solar cells as the intermediate recombination layer and investigated the effect of thickness variation from 20 nm to

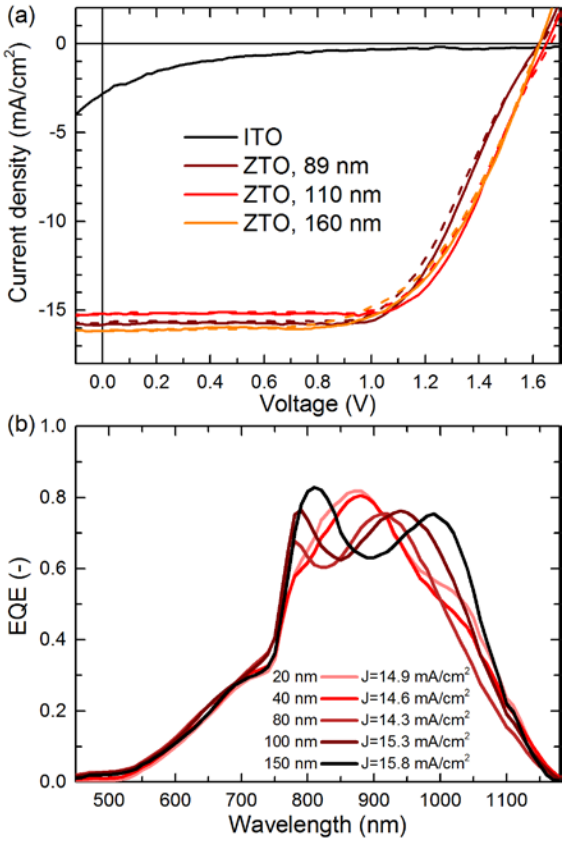

Figure 2 a) J-V curves of monolithic tandem cells with ITO or ZTO recombination layer. Dashed lines are for forward scans (J_{sc} to V_{oc}) and solid lines are for reverse scan (V_{oc} to J_{sc}); b) EQE curves of bottom cells in monolithic tandem devices with different ZTO recombination layer thicknesses.

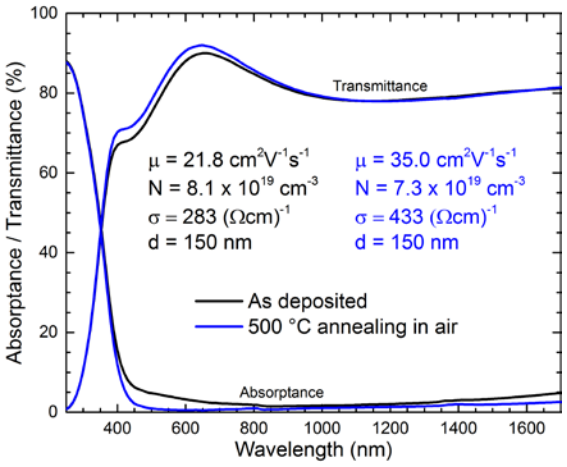

Figure 3 UV-vis-NIR spectrophotometric measurements showing the transmittance and absorptance of a 150 nm thick ZTO layer on glass before and after annealing at 500°C in air. Hall Effect characteristics are also given. μ=mobility; N=carrier density; σ=conductivity; d=thickness.

160 nm. The resulting *J-V* and external quantum efficiency (EQE) characteristics are given in Figure 2, showing rectifying diode-like curves, in contrast to the series resistance limited ITO-based tandem cells. The *J-V* curves with thinner ZTO layers were slightly s-shaped around V_{oc}. However, this problem disappeared with thicker layers, as shown in Figure 2a.

Interestingly, the thickness of this recombination layer had a strong effect on the optical interference pattern in the bottom cell, as revealed by EQE measurements shown in Figure 2b. In our previous study on *planar* perovskite/silicon monolithic tandem cells,[4] the recombination layer thickness did not have such a pronounced interference effect. However, the presence of a mesoscopic layer was found not to be the reason for this difference, as shown in Figure S1 with scaffold-free tandem cells featuring similar interference pattern modifications with thickness. We believe the origin of this phenomenon is found in the different refractive indices of the electron transporting layer (ETL): in our present study, we use TiO_2 which has a refractive index of ~2.5 at 800 nm, compared to 1.9 for the fullerene-based ETL used previously.[4] TCOs such as IZO[15] or ZTO (Figure S2) have refractive indices of about 2 and are therefore better matched to that of the fullerene than TiO_2, as shown in Figure S1b. The larger index contrasts between the intermediate recombination layer and the ETL might therefore be the origin of strong internal reflections at this interface (shown in Figure S3), resulting in the importance of the recombination layer thickness in the overall device optics. Advanced optical modelling would be necessary to further study the interplay of these layers and fine-tune their properties.

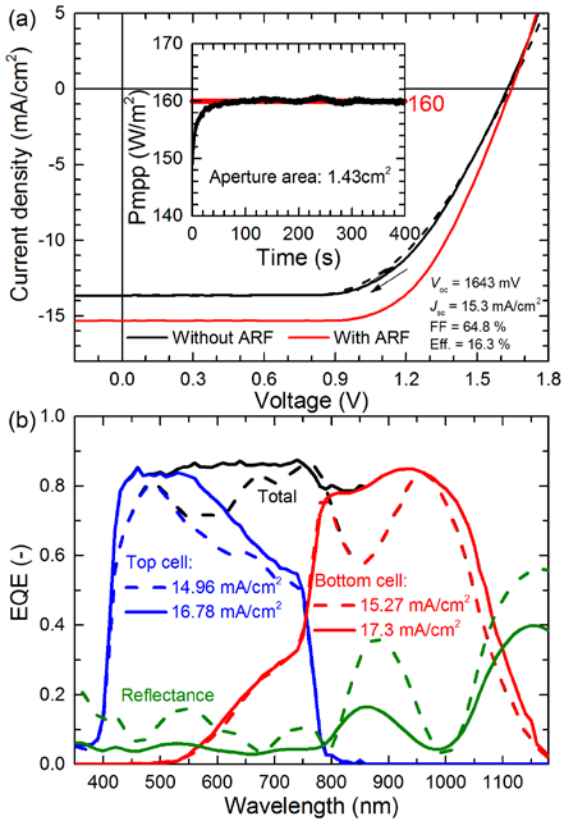

Figure 4 a) J-V measurements of the best performing >1 cm² monolithic tandem with and without antireflective foil (ARF). The inset shows the steady power output measured under maximum power point tracking; b) EQE and total reflectance measurements of the same device as in a), with (solid lines) and without (dashed lines) ARF. The total curve is the sum of the top and bottom cell responses.

In this study, the best monolithic tandem cell with an aperture area of 1.43 cm² showed a V_{oc} of 1643 mV and an initial efficiency of 16.3%, as obtained from *J-V* characteristics, as shown in Figure 4a. During maximum power point tracking, a steady efficiency of 16% was reached (inset to Figure 4a). A smaller cell of 0.25 cm² reached 17.4% (16.4% steady-state; Figure S4). The single-junction semitransparent perovskite solar cells processed as references together with the tandem devices had modest efficiencies around 12% with V_{oc} values of ~1000 mV (Figure S5). The silicon bottom cells V_{oc} has been estimated from devices simulations using Quokka [16] to be around 640 mV. Therefore, the V_{oc} of the tandem was close to the sum of the individual V_{oc} values of the subcells. Clear potential for V_{oc} improvement can be foreseen when comparing the two subcells performances to their state-of-the-art references in literature.[6,8] A boost in V_{OC} of 100-150 mV for the perovskite cell and 50-100 mV for silicon cells with passivated full area contacts could be expected.

The tandem overall performance was mostly limited by series resistance, reducing the fill factor. Further optimization will be required to reduce interfacial resistances in the device, by a better control on the charge carrier density in the recombination layer, and better rear contact processing.

Figure 4b shows the EQE curves for the best large area tandem cell, confirming a closely matched top and bottom cell current generation. The device is however still largely limited by reflection and parasitic absorption, similarly to previous reports.[3–5] Parasitic absorption losses are nevertheless much less prominent compared to the previous work on mesoscopic monolithic tandem cells by Mailoa *et al.*,[2] resulting in a largely improved current. The top cell current is however still limited by absorption in the spiro-OMeTAD hole transporting layer strongly at wavelength < 400 nm. This recurrent problem in this device configuration is an important issue to be solved in the future to further improve current generation in the top cell.[4] The bottom cell could be optically improved by introducing a rear-side texture, in order to increase the near-infrared spectral response.[5]

The tandem process demonstrated here could be applied to higher efficiency silicon bottom cell including standard solar cells made by the diffusion/firing process. In such a case, openings should be made in the SiN of the c-Si cells to contact the doped region. Another more ideal approach would be the use of temperature stable fully passivated contacts.[17] This type of device could rapidly becoming a mainstream high-efficiency silicon commercial technology.[18] Combined with a record top cell,[8,19] monolithic tandem cells could be manufactured at low cost using simple fabrication processes, and performance up to 30% should be practically feasible.[20,21]

To conclude, we have demonstrated the applicability of ZTO as a high-temperature-stable recombination layer, by electro-optical characterization and integration to fully functional devices. This simple junction allowed us to fabricate mesoscopic perovskite/silicon homojunction monolithic tandem solar cells with >16% efficiency. A systematic analysis of the ZTO layer thickness revealed strong resonance effects due to refractive index mismatch with the electron contact and allowed the optimization of the recombination layer thickness for best electrical and optical performance. Further development on the perovskite absorber composition, hole transporting layer transparency and silicon surfaces passivation is expected to result in improved overall performance, with the potential for >30%.

Supplementary material

See supplementary material for the experimental details on device fabrication and characterization, ellipsometric and reflectance data and smaller tandem device performance.

Acknowledgments

The project comprising this work is evaluated by the Swiss National Science Foundation and funded by Nano-Tera.ch with Swiss Confederation financing, by the Swiss Federal Office of Energy, under Grant SI/501072-01. This work has received funding from the European Union's Horizon 2020 research and innovation program under grant agreement No. 653296, as well as from German Federal Ministry for Economic Affairs and Energy (BMWi) under contract no. 0325480A (CHIP). The authors would like to thank S. Kirstein for her help with sample processing and Raphaël Monnard for ellipsometry measurements.

References

1. NREL Efficiency Chart. NREL Efficiency Chart. (2016). Available at: http://www.nrel.gov/ncpv/images/efficiency_chart.jpg. (Accessed: 30th October 2016)

2. Mailoa, J. P. ; Bailie, C. D.; Johlin, E. C. ; Hoke, E. T. ; Akey, A. J.; Nguyen, W. H.; McGehee, M. D.; Buonassisi, T. A 2-terminal perovskite/silicon multijunction solar cell enabled by a silicon tunnel junction. Appl. Phys. Lett. 106, 121105 (2015).

3. Albrecht, S.; Saliba, M. ; Correa Baena, J. P. ; Lang, F. ; Kegelmann, L.; Mews, M.; Steier, L.; Abate, A.; Rappich, J.; Korte, Lars.; et al. Monolithic Perovskite/Silicon-Heterojunction Tandem Solar Cells Processed at Low Temperature. Energy Environ. Sci. 9, 81–88 (2016).

4. Werner, J.; Weng, C.-H.; Walter, A.; Fesquet, L.; Seif, J. P.; De Wolf, S.; Niesen, B.; Ballif, C. Efficient Monolithic Perovskite/Silicon Tandem Solar Cell with Cell Area >1 cm^2. J. Phys. Chem. Lett. 7, 161–166 (2016).

5. Werner, J.; Barraud, L.; Walter, A.; Bräuninger, M.; Sahli, F.; Sacchetto, D.; Tétreault, N.; Paviet-Salomon, B.; Moon, S.-J.; Allebé, C.; et al. Efficient Near-Infrared-Transparent Perovskite Solar Cells Enabling Direct Comparison of 4-Terminal and Monolithic Perovskite/Silicon Tandem Cells. ACS Energy Lett. 474–480 (2016). doi:10.1021/acsenergylett.6b00254

6. Battaglia, C.; Cuevas, A.; De Wolf, S. High-efficiency Crystalline Silicon Solar Cells: Status and Perspectives. Energy Environ. Sci., 9, 1552-1576 (2016). doi:10.1039/C5EE03380B

7. Yang, W. S.; Noh, J. H.; Jeon, N. J.; Kim, Y. C.; Ryu, S.; Seo, J.; Seok, S.Il. High-performance photovoltaic perovskite layers fabricated through intramolecular exchange. Science, 348, 1234–1237 (2015).

8. Saliba, M.; Matsui, T.; Seo, J.-Y.; Domanski, K.; Correa-Baena, J.-P.; Nazeeruddin, M. K.; Zakeeruddin, S. M.; Tress, W.; Abate, A.; Hagfeldt, A.; Grätzel, M. Cesium-containing Triple Cation Perovskite Solar Cells: Improved Stability, Reproducibility and High Efficiency. Energy Environ. Sci. 9, 1989–1997 (2016).

9. Bi, D. ; Tress, W. ; Dar, M. I. ; Gao, P. ; Luo, J. ; Renevier, C. ; Schenk, K. ; Abate, A. ; Giordano, F. ; Correa-Baena, J.-P. ; et al. Efficient luminescent solar cells based on tailored mixed-cation perovskites. Sci. Adv. 2, e1501170 (2016).

10. Oo, T. Z.; Chandra, R. D.; Yantara, N.; Prabhakar, R. R.; Wong, L. H.; Mathews, N.; Mhaisalkar, S. G. Zinc Tin Oxide (ZTO) electron transporting buffer layer in inverted organic solar cell. Org. Electron. physics, Mater. Appl. 13, 870–874 (2012).

11. Morales-Masis, M.; Dauzou, F.; Jeangros, Q.; Dabirian, A.; Lifka, H.; Gierth, R.; Ruske, M.; Moet, D.; Hessler-Wyser, A.; Ballif, C. An Indium-Free Anode for Large-Area Flexible OLEDs: Defect-Free Transparent Conductive Zinc Tin Oxide. Adv. Funct. Mater. 26, 384–392 (2016).

12. Chiang, H. Q.; Wager, J. F.; Hoffman, R. L.; Jeong, J.; Keszler, D. A. High mobility transparent thin-film transistors with amorphous zinc tin oxide channel layer. Appl. Phys. Lett. 86, 13–16 (2005).

13. Jayaraj, M. K.; Saji, K. J.; Nomura, K.; Kamiya, T.; Hosono, H. Optical and electrical properties of amorphous zinc tin oxide thin films examined for thin film transistor application. J. Vac. Sci. Technol. B 26, 495–501 (2008).

14. Dauzou, F.; Bouten, P.; Dabirian, A.; Leterrier, Y.; Ballif, C.; Morales-Masis, M. Mechanical integrity of hybrid indium-free electrodes for flexible devices. Org. Electron. 35, 136–141 (2016).

15. Morales-Masis, M.; Nicolas, S. M.; Holovsky, J.;

De Wolf, S.; Ballif, C. Low-Temperature High-Mobility Amorphous IZO for Silicon Heterojunction Solar Cells. IEEE J. Photovoltaics 5, 1340–1347 (2015).

16. Fell, A.; Fong, K. C.; McIntosh, K. R.; Franklin, E.; Blakers, A. W. 3-D simulation of interdigitated-back-contact silicon solar cells with Quokka including perimeter losses. IEEE J. Photovoltaics 4, 1040–1045 (2014).

17. Hermle, M.; Feldmann, F.; Eisenlohr, J.; Benick, J.; Richter, A.; Lee, B.; Stradins, P.; Rohatgi, A.; Glunz, S. W. Approaching efficiencies above 25% with both sides-contacted silicon solar cells. 2015 IEEE 42nd Photovolt. Spec. Conf. PVSC 2015 8–10 (2015). doi:10.1109/PVSC.2015.7356219

18. Green, M. A. Commercial progress and challenges for photovoltaics. Nat. Energy 1, 15015 (2016).

19. Li, X.; Bi, D.; Yi, C.; Décoppet, J.-D.; Luo, J.; Zakeeruddin, S. M.; Hagfeldt, A.; Grätzel, M. A vacuum flash-assisted solution process for high-efficiency large-area perovskite solar cells. Science, 8060, 1–10 (2016).

20. Filipic, M.; Löper, P.; Niesen, B.; De Wolf, S.; Krc, J.; Ballif, C.; Topic, M. MALI perovskite/silicon tandem solar cells: characterization based optical simulations. Opt. Express 23, 263–278 (2015).

21. Jiang, Y.; Almansouri, I.; Huang, S.; Young, T.; Li, Y.; Peng, Y.; Hou, Q.; Spiccia, L.; Bach, U.; Cheng, Y.-B.; Green, M.; Ho-Bailie, A. Optical Analysis of Perovskite/Silicon Tandem Solar Cells. J. Mater. Chem. C 4, 5679–5689 (2016).